Available online at www.sciencedirect.com
SCIENCE DIRECT
Polymer 46 (2005) 10202–10213
polymer
www.elsevier.com/locate/polymer

# Mechanical and morphological anisotropy in injection molding of thermotropic liquid crystalline copolyesters

Stanley Rendon[a], Wesley R. Burghardt[a,*], Robert A. Bubeck[b], Lowell S. Thomas[b], Bruce Hart[c]

[a]*Department of Chemical and Biological Engineering, Northwestern University, Evanston, IL 60208, USA*
[b]*Michigan Molecular Institute, Midland, MI 48640, USA*
[c]*Saginaw Valley State University, University Center, MI 48710, USA*

Received 24 May 2005; accepted 19 July 2005
Available online 10 August 2005

**Abstract**

Relationships among mechanical properties, degree of molecular orientation and molding conditions are investigated in injection molded plaques fabricated from a 4,4′-dihydroxy-α-methylstilbene (DHαMS)-based thermotropic liquid crystalline copolyester. Wide-angle X-ray scattering (WAXS) patterns reveal bimodal orientation states at most locations in the plaques. One population aligns roughly along the anticipated flow direction while a separate population is generated as a result of transverse stretching associated with diverging streamlines during mold filling. Micro-tensile bars are cut from the plaques both parallel and perpendicular to the filling direction to assess anisotropy in properties. Enhanced molecular orientation and properties 'in-shear' are observed for thinner plaques fabricated at relatively low mold temperatures and melt temperatures slightly above the nominal melting point of the polymer. Injection fill speed is not found to have a significant effect on anisotropy in tensile strength/stiffness. Mechanical properties such as tensile modulus and fracture stress are found to obey a 'universal' correlation with X-ray measurements of molecular orientation projected onto the axis of the testing specimens. These results suggest that even in the presence of complex, spatially heterogeneous orientation states, simple average measures of orientation can provide a robust means of anticipating macroscopic properties.


*Keywords:* Liquid crystalline polymer; Injection molding; Molecular orientation

## 1. Introduction

Thermotropic liquid crystalline polymers (TLCPs) are high performance engineering materials known for their outstanding strength, light weight and high stiffness. TLCPs have inherently low melt viscosities that arise from the spontaneous ordering of rigid rod-like molecules, an attribute that allows for easy processability in operations such as fiber spinning, injection molding and extrusion [1]. Moreover, the excellent specific properties in TLCP fibers are known to depend critically on the overall degree of molecular orientation [2]. Any rational design of TLCP processing thus requires understanding of how processing flow fields influence the net molecular orientation state. While sound fundamental understanding of flow-orientation relationships exists in 'model' flexible main-chain TLCPs [3–11], there are still fundamental open questions in the case of commercial TLCPs (particularly aromatic copolyesters), which bear much greater industrial significance.

Injection molding of TLCPs has received much attention over the last decade, particularly in the fabrication of complex parts where the attainment of strong physical properties in one dimension is a key requirement (e.g. high performance electrical connectors) [12]. The development of high anisotropy during TLCP processing is a critical processing issue known to have significant effects on the physical properties of injection molded parts. Although the concurrence of high tensile properties and highly uni-directional anisotropy is of great benefit in fiber spinning [2], severe anisotropy can be detrimental in injection molded parts, where multidimensional strength and stability are often desired. The rigid nature of the aromatic mesogenic segments in TLCP molecules typically leads to high orientational biases that favor the direction of flow

* Corresponding author. Tel.: +1 847 467 1401; fax: +1 847 491 3728.
*E-mail address:* w-burghardt@northwestern.edu (W.R. Burghardt).

0032-3861/$ - see front matter © 2005 Elsevier Ltd. All rights reserved.
doi:10.1016/j.polymer.2005.07.066

during processing [12–15]. Upon crystallization, such high molecular orientation leads to favorable properties in the direction of flow, but reduced strength in the transverse direction.

Dreher and coworkers [16] have previously characterized relatively narrow injection molded TLCP tensile bars made from Celanese Vectra® copolyester in order to correlate development of chain orientation to mechanical properties. Their study, in which molecular orientation induced during molding was aligned parallel to the specimen axis, showed that tensile modulus increases linearly with the Herman's orientation parameter. Molding of parts with a broad aspect ratio, however, involves greater flow complexity and, consequently, more convoluted orientational states. Due to the lack of fundamentally reliable computational models needed to describe the effect of complex flow kinematics on TLCP orientation, researchers have relied heavily on ex situ characterization methods to investigate molecular orientation in moldings [17–22]. These studies show that depending upon thickness, a layered 'skin-core' morphology frequently results, where shear flow is observed to dominate near the surface while transverse stretching asserts itself near the mid-plane [23–25]. Previous ex situ WAXS studies of molecular orientation on 4,4′-dihydroxy-α-methylstilbene (DHαMS)-based copolyester injection molded plaques also reveal the emergence of complex orientation behavior arising from the competition of inhomogeneous mixed shear and extension [26], generally manifested as bimodal cross-ply orientation states. Shear typically asserts increasing influence with decreasing sample thickness. Similar bimodal character has also been identified in steady isothermal channel flows of DHαMS as well as other commercial TLCPs [27,28], suggesting that the kinematic concepts elucidated by the more idealized extrusion flows also underlie orientation development in the more complex transient non-isothermal case of injection molding.

The combination of complex flow kinematics and thermal histories during injection molding of TLCPs can lead to very complicated distributions of molecular orientation in finished products. Indeed, much of the available literature demonstrates how the distribution of orientation and properties in injection molded TLCPs is extremely sensitive to processing parameters used during molding [29–39]. The potential for highly anisotropic mechanical properties in LCPs motivates better elucidation of how molding geometry and conditions impact the orientation state, and thus the spatial distribution of mechanical properties. This study reports characterization of properties and orientation in molded DHαMS copolyester plaques, subject to systematic variation of thicknesses and processing conditions. Past observations that mechanical properties obey a universal relationship with orientation in the case of uniformly drawn TLCP fibers [2,40] beg the question whether such 'universality' may also be found in the more complex processing case of injection molding, where more complicated orientation states are found [21,26]. In this study, we address this fundamental question through mechanical testing of tensile specimens cut from plaques both parallel and perpendicular to the filling direction in order to assess the anisotropy in properties. Using a suitably defined metric of orientation, our results indeed confirm a strong correlation between mechanical strength or stiffness and X-ray scattering measurements of molecular orientation.

## 2. Experimental

### 2.1. Material

The nematic TLCP used in these studies is an aromatic copolyester containing 4,4′-dihydroxy-α-methylstilbene (DHαMS) as the mesogen and a terephthalate/isophthalate/2,6-naphthalenedicarboxylate molar ratio of 65/10/25; details are available elsewhere [26,41]. This TLCP displays a broad DSC melting endotherm ranging from 235 to 310 °C, with a nominal melting temperature of approximately 280 °C. The onset of degradation occurs at temperatures above 405 °C.

### 2.2. Injection molded plaques

Injection molded DHαMS plaque samples with dimensions of 76.2 by 76.2 mm were fabricated using a Boy 30T2 injection molding machine with injection speed, mold and melt temperature control. A variable thickness insert mold with polished faces and a 'coat hanger' gating was used to generate plaques thicknesses of 3.2, 1.6, and 0.8 mm. 'Fast' fill times of 1 s were typically utilized with some additional molding performed at a 'slow' 5 s. Plaques were fabricated at mold temperatures of 45 and 90 °C while four barrel temperature settings of 250, 275, 300, and 325 °C were used. These corresponded to melt temperatures of 245, 270, 290, and 315 °C, respectively, as determined by using a thermocouple inserted into the melt.

Representative injection molded plaques with a 'coat-hanger' gating are illustrated in Fig. 1(a) and (b). WAXS patterns were collected along seven different line scans across the entire plaque in order to characterize molecular orientation. Three profiles were measured along the filling direction, one along the centerline of the plaque and two off-axes from the centerline spaced symmetrically 20 mm apart. The remaining four profiles were measured laterally at four axial locations spaced symmetrically 16 mm apart. The spacing and location of each line scan were selected to allow correlation of orientation profiles to mechanical measurements of tensile bar specimens cut parallel and transverse to the mold filling direction. X-ray scattering images were collected at 3-mm increments using a motorized $x$–$y$ translation stage. WAXS experiments were conducted at DND-CAT (Sector 5BM-D) of the Advanced Photon

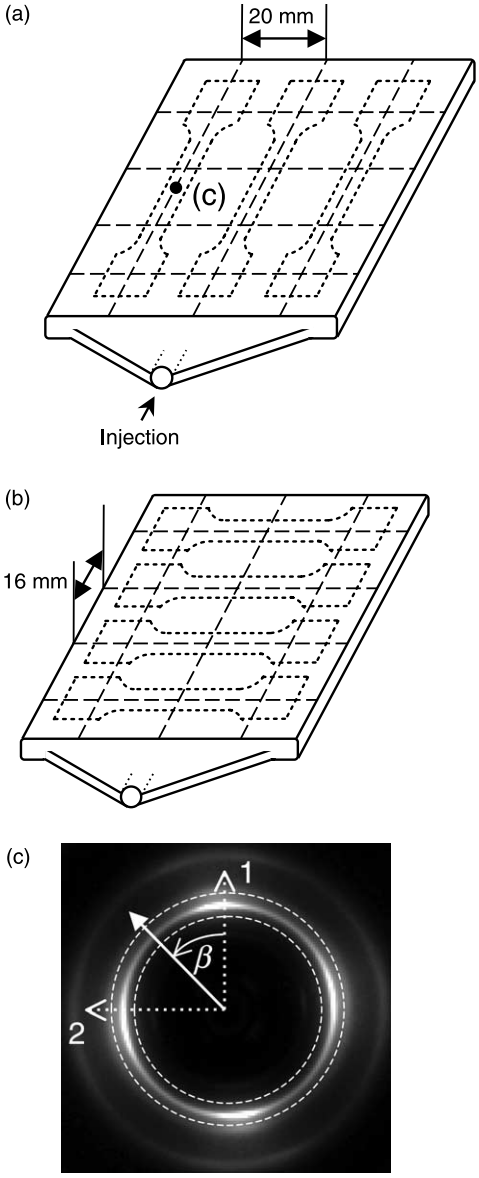


Fig. 1. Schematic representation of injection molded DHαMS plaques illustrating the micro-tensile bar specimen geometry cut: (a) Parallel and (b) perpendicular to the primary injection direction. Dashed lines (– – –) illustrate locations where WAXS measurements were made. (c) Representative X-ray scattering pattern collected at a position off axis to the centerline of a 3.2 mm thick plaque sample made using fast fill, with melt and mold temperatures of 245 and 90 °C, respectively. The azimuthal angle, $\beta$, is measured away from the vertical filling direction. The white dashed circles define the angular $q$-range of intensity used for computing azimuthal scans.

Source at Argonne National Laboratory, using a photon energy of 20 keV (0.62 Å). Guard slits were used to define a square incident X-ray beam with at 1 mm$^2$ cross-section. X-ray scattering patterns with 512×512 pixel resolution were collected using a MarCCD detector with 30 s exposure times.

Similar to previous findings by Rendon and co-workers [26], WAXS patterns frequently show the presence of two sets of nematic crystalline reflections indicating a bimodal distribution of orientation where mixed shear and extension during mold filling lead to populations of orientation parallel and perpendicular to the local filling direction. This is illustrated in a 2D scattering pattern collected along an off-centerline region of a 3.2 mm thick plaque (Fig. 1(c)). This pattern clearly shows diffraction peaks concentrated along both the equator and meridian, which translate to orientational contributions due to shear flow and transverse extension, respectively. It is presumed that this bimodal 'cross-ply' orientation originates from shear flow dominance near the 'skin' surface layer, while transverse extensional flow dominates near the 'core' mid-plane region [26]. (In applying the widely used 'skin-core' terminology, we argue that the population of orientation parallel to the flow direction (as revealed by X-ray scattering) is not solely a superficial surface effect, but rather that 'skin' layers are regions of non-negligible finite thickness near the mold surface in which strong shear gradients dominate, leading to average orientation along the filling direction [26]).

### 2.3. Mechanical characterization

Tensile measurements were carried out on micro-tensile bars machined from the plaques in directions both parallel and perpendicular to the nominal flow direction using a computer programmed end mill. The milling machine was programmed to cut three identical tensile samples parallel to, or four samples perpendicular to, the principal filling direction, as per Fig. 1. The micro-tensile bars were tested at a deformation rate of 1.27 mm/min using an Instron Model 1125 test frame with MTS ReNew© Upgrade Package equipped with an MTS Model 632.29E30 Option 012 extensometer. The standard ASTM D-638 'Standard Test Method for Tensile Properties of Plastics' [42] was used as a guide, but tensile testing procedures were adapted to the specimen dimensions used for this study. An average of five replicates was reported as the final value.

### 2.4. X-ray data analysis

In the case of uniformly drawn TLCP fibers, where one expects a uniaxial distribution of molecular orientation about the fiber axis, X-ray data are usually analyzed to extract an 'order parameter' [26–28]. However, the implicit assumption of uniaxial symmetry in such analyses is untenable in the case of injection molded plaques given the complexity of the orientation states revealed in X-ray scattering patterns (Fig. 1(c)). Instead, we adopt an analysis scheme that directly characterizes anisotropy in the 2D X-ray scattering pattern through the extraction of azimuthal intensity scans over a narrow range of $q$-space and subsequently computing the second moment tensor of the intensity distribution [26–28]. Analysis of X-ray patterns was performed using the software package Fit2D [43]. Fig. 1(c) depicts the range of azimuthal intensity used for all plaque samples. Background intensity sources (e.g. air, detector, etc.) contributing to an isotropic background in the

scattering patterns are removed through careful selection of a baseline intensity value, which is subtracted from all azimuthal scans for individual plaque samples. For each plaque thickness, this baseline value is generally taken to be the lowest intensity observed in the azimuthal scan that displays the highest degree of molecular orientation.

The degree of molecular alignment in a scattering pattern can be characterized by representing each point in the azimuthal scan by the unit vector **u**, such that $u_1 = \cos\beta$ and $u_2 = \sin\beta$, where $\beta$ is the azimuthal angle, measured away from the filling direction (Fig. 1(c)). A weighted average of the second moment tensor of **u** provides a measure of the average orientation in the scattering pattern:

$$\langle \mathbf{uu} \rangle = \begin{bmatrix} \langle u_1 u_1 \rangle & \langle u_1 u_2 \rangle \\ \langle u_1 u_2 \rangle & \langle u_2 u_2 \rangle \end{bmatrix} = \begin{bmatrix} \langle \cos^2\beta \rangle & \langle \sin\beta \cos\beta \rangle \\ \langle \sin\beta \cos\beta \rangle & \langle \sin^2\beta \rangle \end{bmatrix} \quad (1)$$

In this expression, $\langle \ldots \rangle$ represents an average weighted by the azimuthal intensity distribution $I(\beta)$. For example, the 22-component is given by:

$$\langle \sin^2\beta \rangle = \frac{\int_0^{2\pi} \sin^2\beta I(\beta) \mathrm{d}\beta}{\int_0^{2\pi} I(\beta) \mathrm{d}\beta} \quad (2)$$

The difference in the principal eigenvalues of $\langle \mathbf{uu} \rangle$ yields an anisotropy factor (AF) expressed as:

$$\mathrm{AF} = \lambda_1 - \lambda_2 = \sqrt{\left(\langle u_1 u_1 \rangle - \langle u_2 u_2 \rangle\right)^2 + 4\langle u_1 u_2 \rangle^2} \quad (3)$$

By this definition, perfect orientation (in any direction) leads to AF = 1, while an isotropic sample yields AF = 0. The eigenvectors of $\langle \mathbf{uu} \rangle$ indicate the average direction of molecular orientation. Noting that rodlike molecules scatter normal to their axes (a characteristic which is preserved upon crystallization for the reflections studied here), the average orientation direction is characterized by the eigenvector associated with the smaller of the two principal values.

At certain locations on the plaque, we adopt more specialized definitions of anisotropy factor. Given the symmetry of the molding flow, patterns collected along the centerline should align along the 1- and 2-axes, such that the off-diagonal element $\langle u_1 u_2 \rangle = 0$. Under these conditions, we define a 'centerline' anisotropy factor according to:

$$\mathrm{AF}_{\mathrm{centerline}} = \langle u_2 u_2 \rangle - \langle u_1 u_1 \rangle = \langle \sin^2\beta \rangle - \langle \cos^2\beta \rangle \quad (4)$$

This convention results in values of the anisotropy factor that approach +1 for perfect orientation along the flow direction, while −1 corresponds to perfect orientation transverse to the flow direction. It must be borne to mind that this anisotropy factor, as is the case for all bulk measurements of molecular orientation, reflects not just a local distribution of molecular orientation around the director, but also a distribution of director orientations in the sample [44]. In particular, in these plaque samples, these anisotropy factors represent averages through the whole sample thickness, including both 'skin' and 'core' regions [26,27].

A separate specialized definition of anisotropy was used to correlate molecular orientation to mechanical data obtained from experiments on micro-bar tensile specimens cut parallel and transverse to the nominal flow direction. Here, the 'specimen' anisotropy factor is defined differently for each of the two tensile measurement directions:

$$\mathrm{AF}_{\mathrm{specimen}} = \begin{cases} \langle \sin^2\beta \rangle - \langle \cos^2\beta \rangle & \text{Samples} \parallel \text{to filling direction} \\ \langle \cos^2\beta \rangle - \langle \sin^2\beta \rangle & \text{Samples} \perp \text{to filling direction} \end{cases} \quad (5)$$

These definitions only involve the diagonal elements of $\langle \mathbf{uu} \rangle$, even though the off-diagonal component may be non-zero away from the centerline. This reflects the expectation that samples tested along the 1- or 2-axes will yield properties that reflect the projection of orientation onto these axes. Eq. (5) is defined so as to yield positive measures of $\mathrm{AF}_{\mathrm{specimen}}$ when the TLCP molecules are highly aligned along the specimen axis. As shown in Fig. 2, the same scattering pattern will yield both positive and negative $\mathrm{AF}_{\mathrm{specimen}}$ values depending on the orientation of the specimen. Because mechanical characterization experiments yielded single values of tensile modulus ($E$) and fracture stress ($\sigma_f$) averaged over several individual test specimens, we also elected to describe anisotropy through a single value averaged over a 12 mm region centered along the neck region of each tensile bar specimen. This allows a single averaged value of the degree of molecular orientation to be correlated to tensile properties of each individual test specimen.

## 3. Results and discussion

### 3.1. Orientation distributions in injection molded plaques

The 2D distributions of orientation in these square plaques made from the DHαMS-copolyester are comparable to preliminary studies of orientation in smaller, rectangular plaques of this same polymer [26]. While this earlier study sought to establish connections between orientation states observed in injection molding and isothermal channel flows, here we shift emphasis to a much broader parametric study of process conditions, in addition to our goal of establishing direct connections between mechanical properties and complex bimodal orientation states. We begin by surveying molecular orientation results that provide a basis for comparison with mechanical characterization results from tensile specimens.

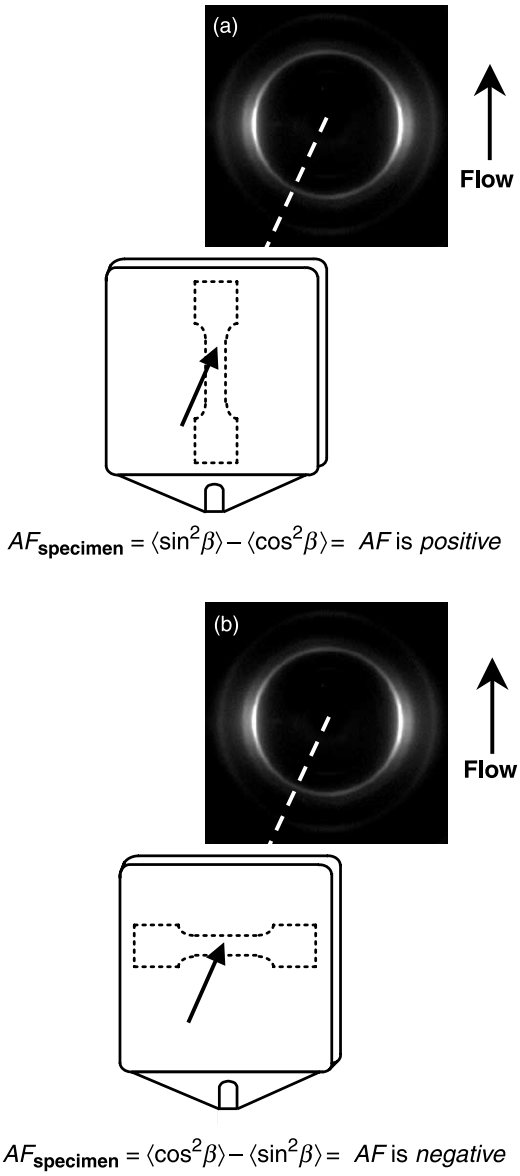


Fig. 2. Representative X-ray scattering patterns collected at a specific plaque location showing identical molecular orientation states for two different micro-tensile bar specimen orientations. (a) Specimen cut parallel to the flow direction displays strong orientation along the filling direction with an anisotropy factor described by $\langle \sin^2\beta \rangle - \langle \cos^2\beta \rangle$, which yields an $AF_{specimen}$ value approaching +1. (b) Specimen cut in the transverse direction displays weak transverse orientation with an anisotropy factor described by $\langle \cos^2\beta \rangle - \langle \sin^2\beta \rangle$, which yields an $AF_{specimen}$ value approaching −1.

### 3.1.1. Effect of mold thickness

The role of mold thickness on the 2D development of orientation in molded plaques was examined through vector plot constructs (Fig. 3(a)–(c)) that survey the local average molecular orientation using the second moment tensor analysis described by Eqs. (1)–(3). The mean orientation direction is given by the axis of each vector, while the strength of the anisotropy is proportional to the length of the vector. An orientation map for the thickest plaque sample (Fig. 3(a)) shows clear consequences of the underlying bimodal orientation distribution; here the transverse population of orientation dominates over shear such that the average orientation direction is actually perpendicular to the filling flow over most of the center region of the plaque. The axial distribution of orientation along the centerline of this 3.2 mm thick plaque (Fig. 3(d)) confirms these observations with values of $AF_{centerline}$ that rapidly decrease from positive to negative downstream of the gate entry region of the plaque. Thinner plaques (1.6 and 0.8 mm) on the other hand exhibit enhanced orientation along the flow direction (Fig. 3(b)–(c)) with $AF_{centerline}$ values that remain positive over most of the plaque length (Fig. 3(d)). In all cases, anisotropy ultimately becomes strongly negative due to the presence of a stagnation point at the end of the mold cavity [26]. The enhancement in anisotropy as a function of decreasing mold thickness reflects the increasing dominance of shear-flow kinematics over transverse extension, in accord with previous findings on similar injection molded DHαMS plaques [26]. The higher relative importance of shear in thin plaques is expected to reduce the thickness of the 'core' (transverse orientation) relative to that of the 'skin'.

### 3.1.2. Effect of melt temperature

Prior studies on this DHαMS copolyester suggest a strong dependence of orientation on melt temperature [26]. Comparison of centerline orientation distributions (Fig. 4) for plaques made at different melt temperatures reveals that transverse orientation states are more readily achieved at the lowest (245 °C) and highest (315 °C) melt temperatures. At melt temperatures slightly above (290 °C) and below (270 °C) the nominal melting point (mp) of the polymer however, the data suggest that molecular orientation follows the mold filling direction much more closely throughout the length of the plaque. Initially all curves display positive anisotropy (presumed to originate from the inherent orientation generated at the injection gate). Further downstream the data appear to 'collapse' into a very narrow range of $AF_{centerline}$ values over the axial region of 32–40 mm near the middle section of the plaque. Beyond this point, the anisotropy begins to decrease towards negative values more rapidly for the case of plaques molded at melt temperatures of 245, 270, and 315 °C. At 290 °C, the data distinctively show a positive increasing slope that ultimately changes direction beyond 62 mm from the gate. Under these conditions, the data clearly show how molecular orientation along the flow direction is most easily maintained at temperatures slightly above the nominal melting point of the polymer.

### 3.1.3. Effect of mold temperature

Axial distributions of molecular orientation (Fig. 5) suggest that the impact of mold temperature on the centerline anisotropy of a molded plaque is sensitive to both the thickness as well as melt temperature used during processing. Comparison of centerline anisotropy at a

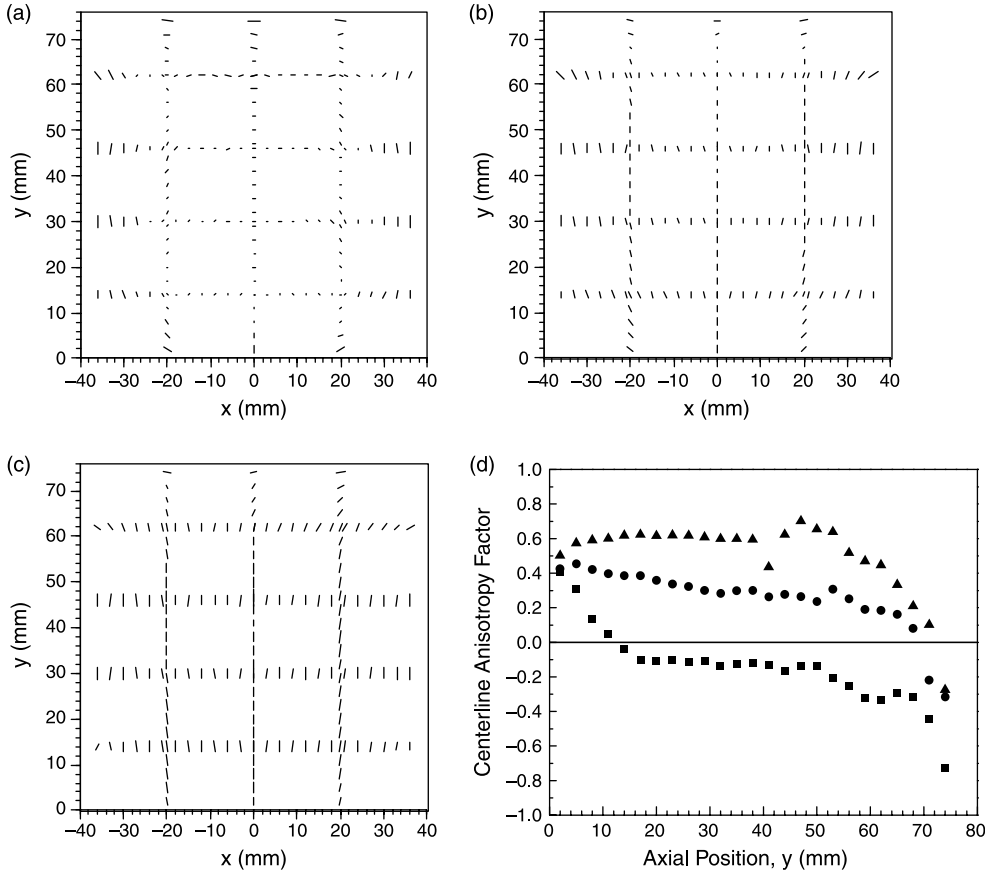


Fig. 3. Vector plots describing the 2D distribution of molecular orientation in DHαMS injection molded plaques, using the second moment tensor description of the anisotropy factor (Eq. (1)) and average orientation direction. The length of the lines reflects the strength of the orientation while the direction is representative of the orientation angle relative to the flow direction. Plaques were all made at constant fast fill times, melt/mold temperatures of 270 °C/45 °C, with thicknesses of: (a) 3.2 mm, (b) 1.6 mm, and (c) 0.8 mm. (d) Corresponding centerline anisotropy factor ($AF_{centerline}$) as a function of axial position computed using Eq. (4): (■) 3.2 mm thick, (●) 1.6 mm thick, and (▲) 0.8 mm thick.

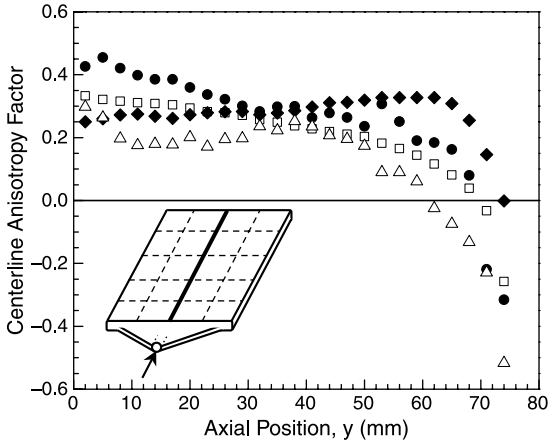


Fig. 4. Effect of melt temperature on the axial distribution of DHαMS copolyester molecular orientation in injection molded plaques: (□) 245 °C, (●) 270 °C, (◆) 290 °C, and (△) 315 °C. Plaques were fabricated under conditions of constant fast fill time, thickness = 1.6 mm, and mold temperature = 45 °C.

constant melt temperature of 290 °C (closed and open triangles) shows that the effects of mold temperature on orientation are increasingly muted as mold thickness decreases. While the thickest plaque (Fig. 5(a)) promotes higher $AF_{centerline}$ values at a mold temperature of 90 °C relative to 45 °C, the thinnest plaque (Fig. 5(c)) exhibits almost identical centerline profiles at these two mold temperatures indicating that at this reduced thickness there is little dependence of orientation on mold temperature. At an intermediate thickness of 1.6 mm (Fig. 5(b)), the influence of mold temperature on orientation is still observed but is less pronounced relative to the thicker 3.2 mm plaque.

While the effects of mold temperature on centerline anisotropy are mitigated as plaque thickness is reduced, the role of melt temperature on orientation is actually far more dramatic at the higher and lower mold thicknesses. As anticipated from Fig. 4, Fig. 5(b) shows that melt temperatures of 245 and 290 °C lead to similar orientation distributions in the 1.6 mm thick plaques (except near then end where transverse extension ultimately leads to a flipping of orientation). Conversely, Fig. 5(a) and (c) shows that

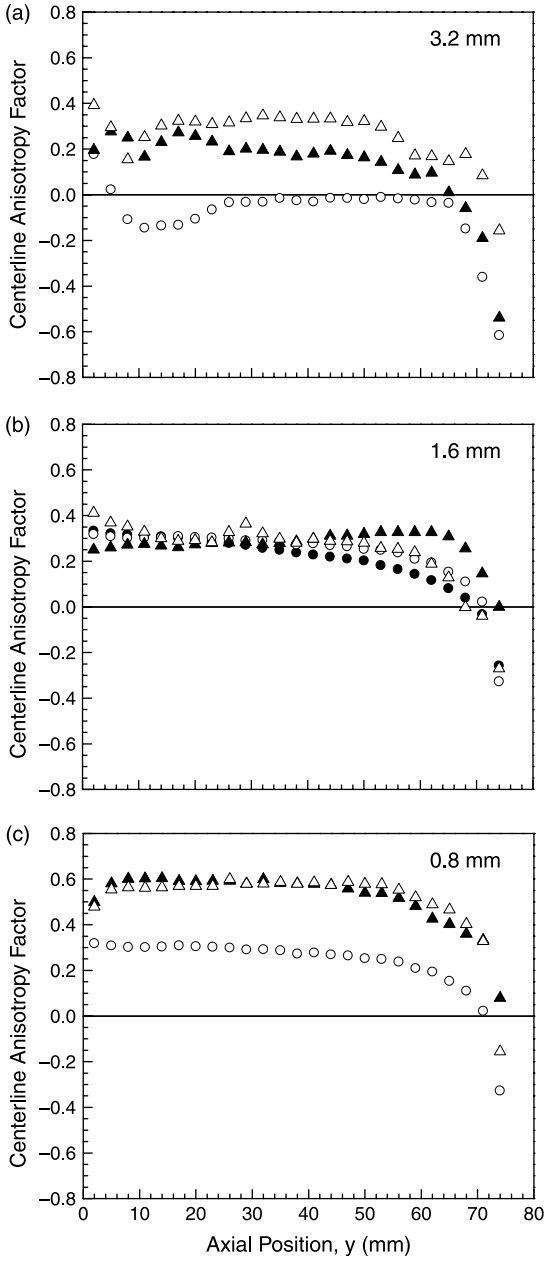


Fig. 5. Effect of mold temperature on the axial distribution of DHαMS copolyester molecular orientation in injection molded plaques with thicknesses of: (a) 3.2 mm, (b) 1.6 mm, and (c) 0.8 mm, made at the following mold/melt temperatures: (●) 45/245 °C, (○) 90 °C/245 °C, (▲) 45/290 °C, and (△) 90/290 °C. All plaques were fabricated under conditions of constant fast fill times.

lower melt temperatures lead to a dramatic reduction in the overall degree of orientation for both thicker and thinner molds. In the 'thick' 3.2 mm plaque (Fig. 5(a)), centerline anisotropy factor profiles are actually negative over most of the plaque length, consistent with reports of increased susceptibility to transverse extension in molding and channel flows at lower melt temperatures [26]. Interestingly similar results are found for the thinnest samples (Fig. 5(c)), although here the centerline anisotropy factor remains positive, in keeping with previously noted trends towards higher degrees of orientation along the filling direction with decreasing sample thickness.

### 3.1.4. Effect of injection speed

Fig. 6 shows the role of fill speed on the evolution of centerline orientation for two plaque thicknesses with mold and melt temperature kept constant. At these molding conditions, $AF_{centerline}$ profiles remain positive for all axial locations; however, the significantly lower anisotropy in the thicker sample demonstrates again how competition between shear and transverse extension reduces overall orientation in thicker samples. Slow fill times (closed symbols) yield higher $AF_{centerline}$ values compared to fast fill times (open symbols). The slower injection speed may allow for greater solidification at the surface during filling leading to a thinner 'effective' thickness as filling proceeds, resulting in higher anisotropy.

## 3.2. Correlation of molecular orientation to mechanical properties in molded plaques

It is clear that processing conditions can have a significant impact on the degree of molecular orientation in injection molded DHαMS plaques. The final mechanical properties of the molded plaque will depend upon how these processing parameters and the resulting anisotropy affect the macroscopic orientation during mold filling. This anisotropy can be extreme; in DHαMS, tensile properties can range for tensile moduli from $E=2$ to 25 GPa with corresponding fracture stresses of $\sigma_f=20$–125 MPa, for the particular case of 0.8 mm thick plaques processed at melt and mold temperatures of 290 and 45 °C, respectively [45]. These values, however, represent a fairly extreme set of

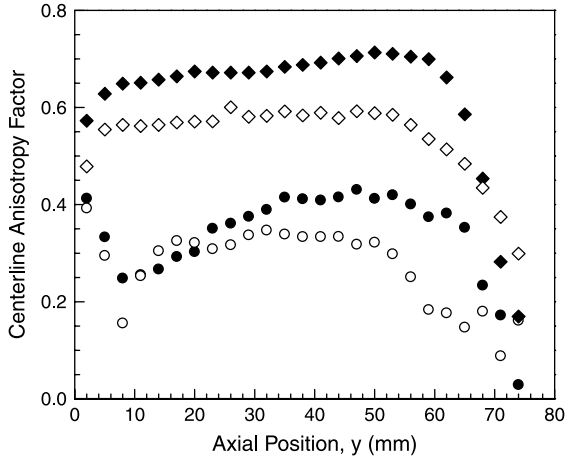


Fig. 6. Effect of injection speed on the axial distribution of DHαMS copolyester molecular orientation in injection molded plaques made at the following thickness/fill speed: (●) 3.2 mm/slow fill, (○) 3.2 mm/fast fill, (♦) 0.8 mm/slow fill, and (◇) 0.8 mm/fast fill. All plaques were fabricated under conditions of constant melt temperature = 290 °C and mold temperature = 90 °C.

conditions where properties are dominated primarily by the 'skin' layer formed under the influence of shear flow.

In order to explore the relationship between tensile properties and molecular orientation in DHαMS plaques molded over the entire range of processing conditions and thicknesses studied here, comprehensive 'master' graphs of tensile modulus and fracture stress as a function of specimen anisotropy factor ($AF_{specimen}$) have been prepared (Fig. 7). The tensile data are comprised of average measurements of tensile properties from all ASTM specimens cut from molded plaques. For a given specimen, the sign of the anisotropy factor is primarily determined by the direction it was cut: Samples cut parallel to the fill direction usually show positive values, and vice-versa. However, samples tested along the primary flow direction occasionally show negative values of anisotropy as a result of processing conditions biasing the orientation towards the transverse direction; this would be true, for instance, for the plaque presented in Fig. 3(a).

The observed increase in tensile modulus with increasingly positive anisotropy (Fig. 7(a)) is similar to data for melt drawn HBA/HNA random copolyester TLCP filaments by Garg and Kenig [40]. The corresponding values for peak stress at fracture versus $AF_{specimen}$ are also shown (Fig. 7(b)), and with some scatter, demonstrate a similar strong connection to orientation over the wide range of sample thickness and process conditions studied. The weaker dependence of fracture stress as a function of $AF_{specimen}$ relative to modulus presumably arises from the fact that stress at break is much more greatly influenced by defects and defect population than is modulus.

Because melt temperature and mold thickness are known to have a significant effect on the degree of molecular orientation, and thus on mechanical properties, we have isolated these two processing variables in cross plots of tensile properties versus anisotropy factor (Fig. 8). The higher melt temperature data (closed symbols) are concentrated at the extremes of the positive and negative $AF_{specimen}$ axis range, while the lower melt temperatures are associated with less extreme anisotropy values. The data show that strong molecular orientation resulting from processing at the higher melt temperature of 290 °C leads to large values of moduli ($E \geq 9$ GPa) measured in that direction. At this same melt temperature all tensile

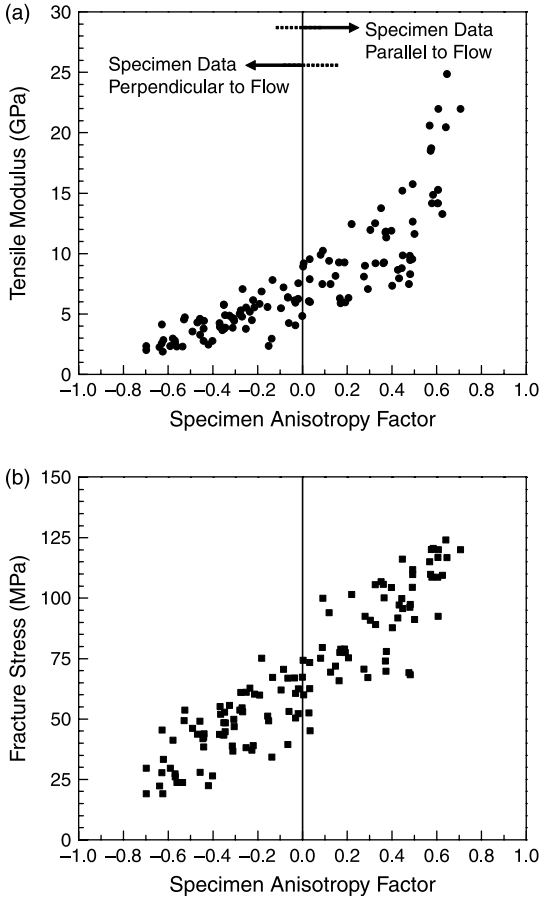


Fig. 7. Comprehensive cross-plots of (a) tensile modulus and (b) fracture stress as a function of specimen anisotropy factor ($AF_{specimen}$) for ASTM specimens cut parallel and perpendicular to the principal flow direction of DHαMS plaques made over the entire range of processing conditions studied.

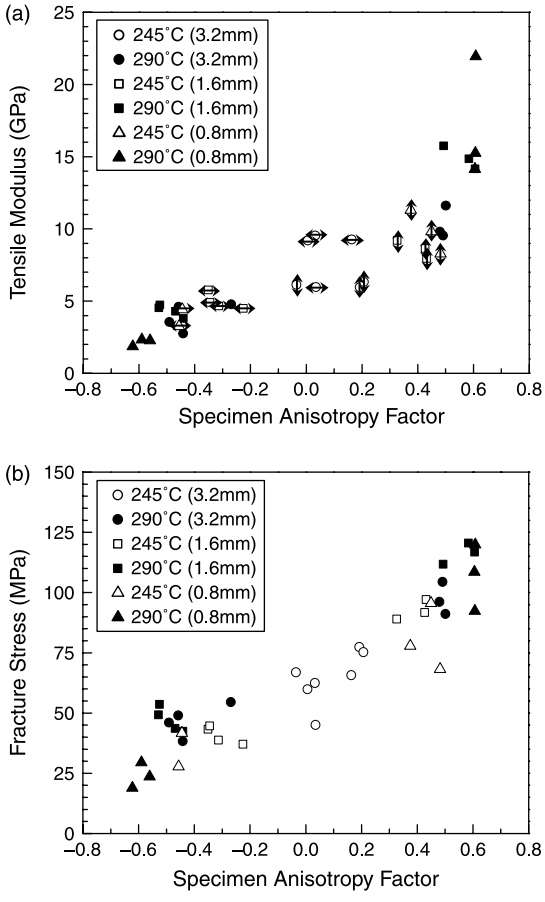


Fig. 8. Cross-plots of (a) tensile modulus and (b) fracture stress as a function of specimen anisotropy factor ($AF_{specimen}$) isolating the effects of melt temperature and plaque thickness. Arrows on symbols indicate direction in which tensile measurements were performed. Data are presented for plaques molded under conditions of constant fast fill times and mold temperature = 90 °C.

specimens cut perpendicular to the nominal flow direction are characterized by weak properties with moduli values falling below 5 GPa over the range of $AF_{specimen} \leq -0.25$. These observations are also reflected in a fracture stress-AF cross plot provided in Fig. 8(b).

The role of mold thickness can be discerned by closer inspection of the data in Fig. 8. Within both populations of data (245 and 290 °C melt temperature), the thin samples (triangles) tend toward more extreme (positive or negative) values of $AF_{specimen}$, reflecting the general observation that thinner samples lead to greater degrees of orientation. Previous investigators have also observed significant increases in mechanical anisotropy along the mean molecular orientation direction associated with decreasing plaque thickness [13,21]. It is clear that any probe of macroscopic properties in either plaque direction (Fig. 2) will be directly sensitive to changes in the relative thickness of the 'skin-core' layers; as discussed earlier, sample thickness provides the most direct control over the competition between shear and extension which leads to the characteristic bimodal states. For the thick samples fabricated at the lower melt temperature (open circles), the average orientation state is nearly isotropic. In fact, this is one test condition in which transverse-cut samples exhibit positive $AF_{specimen}$, while one parallel-cut specimen exhibits negative $AF_{specimen}$.

As discussed earlier, Garg and Kenig [40] demonstrated that tensile modulus increases sharply over increasing values of the Herman's orientation parameter for HBA/HNA random copolyester TLCP fibers subjected to varying melt drawing ratios. The elongational deformation during drawing led to simple uniaxial orientation states in those oriented fibers. Even for the complex, bimodal orientation fields generated by the complex flow kinematics in injection molding, these data demonstrate that a similar correlation exists provided that a suitable measure of orientation is defined. Even when the average orientation direction in the sample is not coincident with the testing axis, we find that a projection of molecular orientation onto the testing axis (Eq. (5)) provides a simple metric that reliably correlates with mechanical properties. This in turn suggests that the properties of spatially heterogeneous moldings may be reliably anticipated once (or if) the factors that govern development of orientation during processing are elucidated.

Although Fig. 7 clearly shows a strong correlation of properties to orientation, the data nonetheless show a notable amount of scatter that is presumed to arise from: (i) Some inherent scatter in tensile measurements and/or (ii) a consequence of bimodal orientation states in molded plaques. While the data spread is small at opposite ends of the $AF_{specimen}$ axis in both moduli and fracture stress (Fig. 7), the distribution becomes much wider at intermediate values of anisotropy. It is precisely in this regime where bimodal skin and core orientation states cancel to yield low overall anisotropy. Since the underlying relationship between anisotropy and modulus is highly non-linear, differences in the distribution of orientation with depth through the sample (i.e. skin vs. core) might lead to more widely varying net mechanical properties even when the average anisotropy is similar. Similar trends have been previously reported by Zulle and co-workers, which show rapidly increasing tensile properties (with some noticeable scatter) as a function of percent skin of individual layers of Vectra® copolyester moldings [35].

### 3.3. Effect of molding parameters on plaque mechanical anisotropy

Results in Figs. 7 and 8 demonstrate that the LCP molecular orientation state is inarguably the essential intermediate link between changes in processing conditions and the ultimately obtained mechanical properties. However, detailed process modeling of orientation development in commercial TLCPs is still a challenging proposition, while detailed characterization of orientation distribution in moldings is too laborious for routine process development studies. In this section, we revert to a coarser view of how process conditions affect the anisotropic mechanical properties of the molded plaques (informed, to be sure, by the molecular orientation results from prior sections). For this purpose, we adopt a more macroscopic viewpoint in which mechanical data from perpendicular and parallel test specimens from a given sample are averaged to yield an overall picture of anisotropy for each plaque as a whole.

#### 3.3.1. Effect of mold thickness, melt temperature and mold temperature

Averaged measurements of tensile modulus made parallel ($E_{\parallel}$) or perpendicular ($E_{\perp}$) to the principal injection direction are seen to depend critically on process variables (Fig. 9(a)–(c)). As anticipated from earlier results, thin plaques lead to the highest anisotropy in mechanical properties, as well as the highest moduli in samples cut parallel to the filling direction (Fig. 9(c)). At each melt temperature, anisotropy in mechanical properties and the modulus parallel to the filling direction decrease with increasing sample thickness. The greater relative importance of transverse extension with increasing sample thickness leads to a larger fraction of material in the transverse orientation state, reducing the overall degree of molecular alignment along the filling direction (Figs. 3 and 5). Earlier data have shown that the combination of lower melt temperatures and thick moldings lead to a flipping in average orientation direction (characterized by negative centerline anisotropy factors in Figs. 3(d) and 5(a)); a similar inversion is found for the thick moldings at the lowest melt temperature (Fig. 9(a)), where a higher modulus is observed in specimens cut perpendicular to the filling direction.

These data further clarify how melt temperature during processing has a strong effect on the resulting mechanical properties. The lowest (245 °C) and highest (315 °C) melt temperatures are generally associated with reduced 'in-

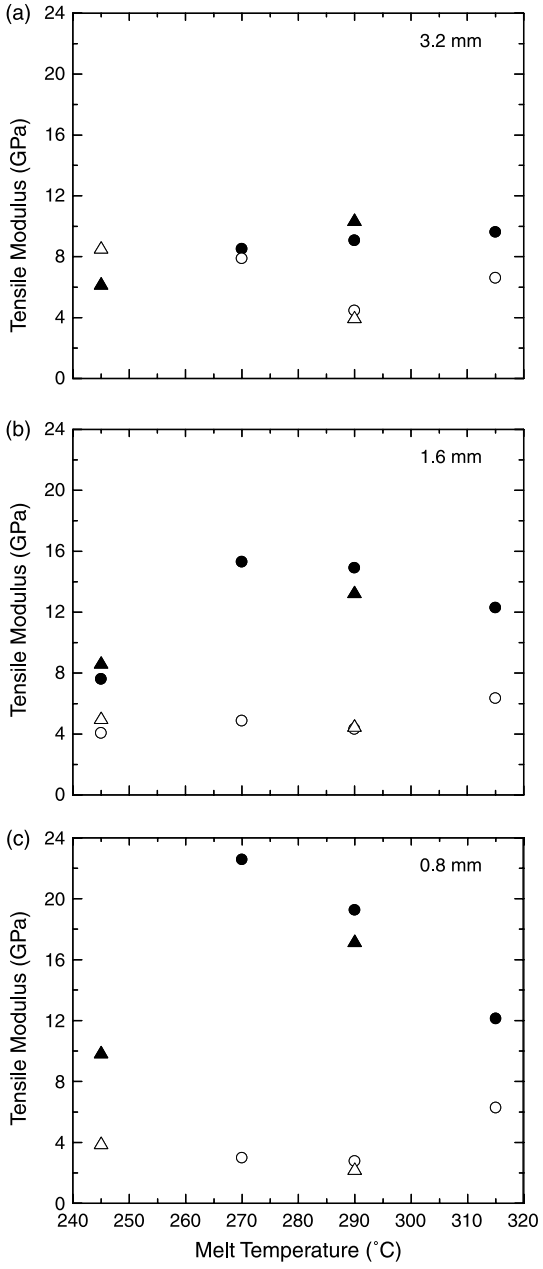


Fig. 9. Plot of tensile modulus as a function of melt temperature for injection molded plaques of varying thickness: (a) 3.2 mm, (b) 1.6 mm, and (c) 0.8 mm. Each data point represents an averaged measure of tensile modulus for ASTM specimens cut either parallel (three specimen average) or perpendicular (four specimen average) to the principal flow direction. Data are presented for samples cut parallel to the flow direction (closed symbols) at mold temperatures of 45 °C (●) and 90 °C (▲) and perpendicular to the flow direction (open symbols) at mold temperatures of 45 °C (○) and 90 °C (△). All plaques were fabricated under conditions of constant fast fill times.

shear' properties and lower mechanical anisotropy. The former is consistent with the increased susceptibility towards transverse stretching found at low melt temperature in previous channel flow and molding studies [26], further amplified here in Figs. 4 and 5. The reduction in anisotropy and $E_{\|}$ at the highest melt temperature resembles previous reports in injection molded polycarbonate/LCP in situ composites containing thermotropic Vectra A950 [46] as well as in other high molecular weight copolyesters containing *p*-hydroxybenzoic acid (PHB) [13]. At any given thickness, the highest strength is generally found for melt temperatures (270 or 290 °C) close to the nominal melting temperature (280 °C) of this DHαMS copolyester. Prior studies on HNA/HBA injection molded copolyester TLCPs also found that optimal tensile properties along the principal flow direction are achieved only at melt temperatures close to the nominal mp of the polymer [36,46]. At very high melt temperatures there is a significant decrease in viscosity which drastically reduces viscous shear stresses generated during mold filling, thus, inducing more relaxation of orientation. Moreover, the susceptibility for polymer degradation at these high temperatures can also contribute to the decrease in mechanical strength. Reduced 'in-shear' mechanical strength resulting from lower operating melt temperatures has been previously associated to either the presence of residual crystallites in the melt [47] or the onset of flow-induced crystallization [48].

The influence of mold temperature on $E_{\|}$ and $E_{\perp}$ in molded plaques appears to be more subtle relative to the effects of thickness and melt temperature (Fig. 9). In all cases where direct comparisons are possible (circles vs. triangles), mold temperature has a weaker effect than the other variable under consideration. At a melt temperature of 290 °C, the two thinner samples show improved 'in-shear' tensile properties at the lower mold temperature. This observation is supported by much of the available literature which suggests that increasing mold temperatures lead to a reduction in 'skin' thickness in molded TLCP plaques [35–37]. Morphological and mechanical studies by Zulle et al. [35] and Suokas et al. [37] on commercial Vectra® copolyester moldings attribute reductions in mechanical strength to variations in relative proportions of the different layers within the cross-sections of molded plaques. Near the nematic melt temperature range, intermediate 'sub-skin' layers aligned 'in-shear' are generated at the expense of the transversely oriented center 'core'. Related to this is the simple fact that the LCP remains in the melt for a longer time at higher mold temperatures, proving increased opportunity for flow-induced orientation to relax prior to melt solidification. The situation reverses at the largest sample thickness where higher mold temperatures lead to improved tensile properties along the filling direction (Fig. 9(a)). It is interesting to note that Fig. 5(a) similarly showed the strongest effect of mold temperature on orientation profiles for the thickest sample, and that the higher mold temperature led to higher overall molecular orientation in this particular case.

### 3.3.2. *Effect of injection speed*

Tables 1 and 2 summarize the effect of fill speed on the mechanical anisotropy and fracture stress ratio computed

for plaques of varying thickness and melt temperature, respectively. Mechanical anisotropy is defined here as the ratio of tensile moduli measured parallel ($E_{\parallel}$) and perpendicular ($E_{\perp}$) to the flow averaged over test specimens measured in each of the two directions; similarly, fracture stress ratio is computed to compare fracture properties in both the flow and transverse directions. While the anisotropy in properties is higher at the lower thickness and higher melt temperature (as expected), the data show a very weak dependence of anisotropy on fill speed. Axial measurements of centerline molecular orientation (Fig. 6) showed enhanced molecular orientation along the filling direction at slower injection rates. While most of the data in Tables 1 and 2 indeed show some increase in anisotropy at slower fill speeds, these differences are small, typically within the range of uncertainty associated with lumping data from all parallel and perpendicular specimens into a single, averaged value. It is interesting to note that flow rate was found to have only a weak effect on molecular orientation measured in isothermal channel flows of this DHαMS copolyester [26]; since changes in flow rate affect shear and extension rates equally, it was postulated that variations in superficial velocity do not fundamentally change the competition between shear and extension the way geometric variables (e.g. sample thickness) do. The lack of a significant effect of fill speed on properties is broadly consistent with these arguments.

## 4. Conclusions

The influence of molding parameters and mold thickness on the anisotropy, 'skin-core' morphology, and mechanical properties in plaques made from a DHαMS-based copolyester have been studied. Molded plaques frequently exhibit bimodal orientation states characterized by two populations of orientation, one roughly aligned with the flow direction and another generally transverse to the flow. The spatially-varying competition between inhomogeneous mixed shear and transverse extension is known to lead to complex bimodal character based on expectations from prior isothermal channel flow studies on DHαMS and other commercial main-chain TLCPs.

Mechanical testing of micro-tensile bar specimens cut parallel and perpendicular to the mold filling direction of molded plaques reveals that tensile modulus and fracture stress are well correlated with the degree of molecular orientation, as described by a specimen anisotropy factor ($AF_{specimen}$) computed from 2D WAXS patterns. Overall, properties are found to follow a 'universal' correlation with anisotropy factor projected onto the axis of the tensile specimens. While the overall relationship is simple, properties of specific samples are found to depend critically on mold thickness and other processing parameters such as melt and mold temperature. Weak dependence of orientation and properties on fill speed during molding is observed. In general, mechanical properties and anisotropy are enhanced at low mold temperatures and at melt temperatures close to the nominal melting point of the polymer. Because anisotropy in orientation and properties is typically aggravated with decreasing mold thickness, there exists a compromise thickness range (in the environs of 1.6 mm) for which reasonable multi-directional properties are obtained. Any unfavorable effects of anisotropy are mitigated (but not eliminated) by off-setting contributions from transverse extension and shear flow in the mold cavity. These results demonstrate even in a complex transient non-isothermal process such as injection molding, it is possible to anticipate macroscopic properties through simple descriptions of average orientation. The universality in properties with orientation observed in this DHαMS-copolyester should prove useful in identifying optimal process conditions for the injection molding of larger size moldings fabricated from TLCPs.

Table 1
Effect of injection speed on the mechanical anisotropy and fracture stress ratio for injection molded DHαMS plaques fabricated at a melt and mold temperature of 290 and 90 °C, respectively, for two different plaque thicknesses

| | Plaque thickness = 0.8 mm | | Plaque thickness = 3.2 mm | |
|---|---|---|---|---|
| Injection speed | Mechanical anisotropy ($E_{\parallel}/E_{\perp}$) | Fracture stress ratio ($\sigma_{\parallel}/\sigma_{\perp}$) | Mechanical anisotropy ($E_{\parallel}/E_{\perp}$) | Fracture stress ratio ($\sigma_{\parallel}/\sigma_{\perp}$) |
| 1 s fill | 7.94 | 4.45 | 2.63 | 2.07 |
| 5 s fill | 7.74 | 4.54 | 2.84 | 2.24 |
| Uncertainty (±) | 0.49 | 0.57 | 0.36 | 0.38 |

Table 2
Effect of injection speed on the mechanical anisotropy and fracture stress ratio for injection molded DHαMS plaques fabricated at a thickness = 3.2 mm and mold temperature = 90 °C, for two different melt temperatures

| | Melt temperature = 245 °C | | Melt temperature = 290 °C | |
|---|---|---|---|---|
| Injection speed | Mechanical ancisotropy ($E_{\parallel}/E_{\perp}$) | Fracture stress ratio ($\sigma_{\parallel}/\sigma_{\perp}$) | Mechanical anisotropy ($E_{\parallel}/E_{\perp}$) | Fracture stress ratio ($\sigma_{\parallel}/\sigma_{\perp}$) |
| 1 s fill | 0.72 | 1.26 | 2.63 | 2.07 |
| 5 s fill | 1.01 | 1.43 | 2.84 | 2.24 |
| Uncertainty (±) | 0.16 | 0.20 | 0.36 | 0.38 |

## Acknowledgements

The assistance of Andrew Bauman and Jennifer Pettengill (SVSU) with mechanical testing is greatly appreciated. We acknowledge financial support from the National Science Foundation Grants DMI-0132519 and DMI-0099542. X-ray experiments were conducted at the DuPont-Northwestern-Dow Collaborative Access Team

(DND-CAT) Synchrotron Research Center located at Sector 5 of the Advanced Photon Source of Argonne National Laboratory. DND-CAT is supported by the E.I. DuPont de Nemours and Co., the Dow Chemical Company, and the National Science Foundation through Grant DMR-9304725 and the State of Illinois through the Department of Commerce and the Board of Higher Education Grant IBHE HECA NWU 96. Use of the Advanced Photon Source was supported by the US Department of Energy, Basic Energy Sciences, Office of Energy Research, under Contract No. W-31-102-Eng-38.

## References

[1] Noel C, Navard P. Prog Polym Sci 1991;16(1):55–110.
[2] Donald AM, Windle AH. Liquid crystalline polymers. Cambridge: Cambridge University Press; 1992.
[3] Kim SS, Han CD. Macromolecules 1993;26(12):3176–86.
[4] Kim SS, Han CD. J Rheol 1993;37(5):847–66.
[5] Gillmor JR, Colby RH, Hall E, Ober CK. J Rheol 1994;38(5): 1623–38.
[6] Chang S, Han CD. Macromolecules 1997;30(6):1656–69.
[7] Mather PT, Jeon HG, Han CD, Chang S. Macromolecules 2000; 33(20):7594–608.
[8] Zhou WJ, Kornfield JA, Ugaz VM, Burghardt WR, Link DR, Clark NA. Macromolecules 1999;32(17):5581–93.
[9] Zhou WJ, Kornfield JA, Burghardt WR. Macromolecules 2001; 34(11):3654–60.
[10] Ugaz VM, Burghardt WR, Zhou WJ, Kornfield JA. J Rheol 2001; 45(5):1029–63.
[11] Ugaz VM, Burghardt WR. Macromolecules 1998;31(24):8474–84.
[12] Samulski ET. In: Board NMA, editor. Liquid-crystalline polymers. USA: National Academy Press; 1990 (NMAB-453).
[13] Jackson WJ, Kuhfuss HF. J Polym Sci Pol Chem 1976;14(8):2043–58.
[14] Blundell DJ, Chivers RA, Curson AD, Love JC, Macdonald WA. Polymer 1988;29(8):1459–67.
[15] Kim YC. Polym J 1998;30(8):610–5.
[16] Dreher S, Seifert S, Zachmann HG, Moszner N, Mercoli P, Zanghellini G. J Appl Polym Sci 1998;67(3):531–45.
[17] Ide Y, Ophir Z. Polym Eng Sci 1983;23(5):261–5.
[18] Gogos CG, Huang CF, Schmidt LR. Polym Eng Sci 1986;26(20): 1457–66.
[19] Pirnia A, Sung CSP. Macromolecules 1988;21(9):2699–706.
[20] Bensaad S, Jasse B, Noel C. Polymer 1993;34(8):1602–6.
[21] Heynderickx I, Paridaans F. Polymer 1993;34(19):4068–74.
[22] Jansen JAJ, Paridaans FN, Heynderickx IEJ. Polymer 1994;35(14): 2970–6.
[23] Ophir Z, Ide Y. Polym Eng Sci 1983;23(14):792–6.
[24] Sawyer LC, Jaffe M. J Mater Sci 1986;21(6):1897–913.
[25] Weng T, Hiltner A, Baer E. J Mater Sci 1986;21(3):744–50.
[26] Rendon S, Burghardt WR, New A, Bubeck RA, Thomas LS. Polymer 2004;45(15):5341–52.
[27] Cinader DK, Burghardt WR. J Polym Sci Pol Phys 1999;37(24): 3411–28.
[28] Cinader DK, Burghardt WR. Rheol Acta 2000;39(3):247–58.
[29] Sweeney J, Brew B, Duckett RA, Ward IM. Polymer 1992;33(23): 4901–7.
[30] Turek DE, Simon GP. Polymer 1993;34(13):2763–8.
[31] Green DI, Collins TLD, Davies GR, Ward IM. Polymer 1997;38(21): 5355–61.
[32] Wang YL, Yue CY, Tam KC, Hue X. J Appl Polym Sci 2003;88(7): 1713–8.
[33] Duska JJ. Plast Eng 1986;42(12):39–42.
[34] Zulle B, Demarmels A, Plummer CJG, Schneider T, Kausch HH. J Mater Sci Lett 1992;11(21):1411–3.
[35] Zulle B, Demarmels A, Plummer CJG, Kausch HH. Polymer 1993; 34(17):3628–37.
[36] Nguyen TN, Geiger K, Walther T. Polym Eng Sci 2000;40(7): 1643–54.
[37] Suokas E. Polymer 1989;30(6):1105–12.
[38] Plummer CJG, Wu Y, Davies P, Zulle B, Demarmels A, Kausch HH. J Appl Polym Sci 1993;48(4):731–40.
[39] Plummer CJG, Zulle B, Demarmels A, Kausch HH. J Appl Polym Sci 1993;48(5):751–66.
[40] Garg SK, Kenig S. High modulus polymers, Dekker, New York; 1988.
[41] Bales SE, Hefner RE, Singh R. The Dow Chemical Co., March 25, 1997, US Patent 5,614,599.
[42] 1989 Annual Book of ASTM Standards, 08.01, Plastics, p. 156–76, ASTM, Philadelphia, PA.
[43] Hammersley AP. http://www.esrf.fr/computing/scientific/FIT2D/, ESRF, (last update) April, 2005.
[44] Burghardt WR. Macromol Chem Phys 1998;199(4):471–88.
[45] Bubeck RA, Thomas LS, Burghardt WR, Rendon S, Hexemer A, Hart B. 12th Churchill conference on deformation. Yield Fract Polym 2003;12:155–8.
[46] Chan HS, Leng Y, Gao F. Compos Sci Technol 2002;62(6):757–65.
[47] Lin YG, Winter HH. Macromolecules 1988;21(8):2439–43.
[48] Romo-Uribe A, Windle AH. Macromolecules 1996;29:6246–55.